Journal of Luminescence 132 (2012) 1729–1734

Contents lists available at SciVerse ScienceDirect

Journal of Luminescence

journal homepage: www.elsevier.com/locate/jlumin

Highly selective fluorescent chemosensor for detecting Hg(II) in water based on pyrene functionalized core–shell structured mesoporous silica

Xiaorong Guo [a], Bin Li [a,*], Liming Zhang [b], Yinghui Wang [b]

[a] Key Laboratory of Polyoxometalate Science of Ministry of Education, Faculty of Chemistry, Northeast Normal University, Renmin Street No. 5268, Changchun, Jilin 130024, PR China

[b] Key Laboratory of Excited State Processes, Changchun Institute of Optics, Fine Mechanics and Physics, Chinese Academy of Sciences, Changchun 130033, PR China

ARTICLE INFO

Article history:
Received 10 January 2011
Received in revised form
12 June 2011
Accepted 30 January 2012
Available online 4 February 2012

Keywords:
Hg^{2+}
Fluorescence sensor
Core–shell
Mesoporous silica

ABSTRACT

Novel pyrene functionalized mesoporous core–shell structured silica (denoted as SiO_2@mSiO_2/Py-Si) was designed and synthesized as a highly selective fluorescent chemosensor for detecting Hg^{2+} in water. The core–shell structured silica was prepared by a simple sol–gel process through coating SiO_2 nanospheres with a layer of ordered mesoporous silica. The surface of outer mesoporous silica shell was then further functionalized by the fluorescent chromophore alkoxysilane modified pyrene (Py-Si). XRD data confirmed that the hexagonal ordered mesoporous structure was preserved after functionalization. The chemosensing material successfully exhibited a remarkable "turn on" response toward Hg^{2+} over miscellaneous metal ions. A good linear response towards Hg^{2+} in the concentration range of 10^{-8}–10^{-4} M was constructed with $R^2=0.9913$. Most importantly, a satisfactory detection limit of 3.4×10^{-9} g mL^{-1} (down to ppb level) was obtained, which is 100 times lower than our previous report of covalently grafted Py-OH to the bulk mesoporous silica SBA-15. These results indicated that SiO_2@mSiO_2/Py-Si can be used as a highly selective and sensitive fluorescence sensor for Hg^{2+}.

1. Introduction

Considerable attention has been paid to the design and development of new chemical sensors for selective and sensitive quantification of biologically and environmentally important ion species, especially heavy metal ions. Among harmful heavy metal ions, mercury ion is one of the most prevalent toxic metal ions, and has severe effects on human health and environment because of its severe immunotoxic, genotoxic, and neurotoxic effects [1,2]. Mercury ion has been reported to produce harmful effects at 5 μg L^{-1} in a culture medium [3], which can damage the heart, kidney, stomach, and intestines in human [4–6]. Therefore, mercury pollution is a topic of recent concern, and has sparked interest in the design of new chemical tools and tactics for its detection. To date, several methods and techniques have been used to monitor concentration levels of Hg^{2+} in water samples, such as atomic absorption spectroscopy [7,8], gas chromatography–inductively coupled plasma-mass spectrometry [9], atomic fluorescence spectrometry [10,11], inductively coupled plasma-atomic emission spectrometry [12,13], and reversed-phase high-performance liquid chromatography [14], which can provide limits of detection at parts-per-billion level. However, their wide utilization is largely limited due to their extremely high cost. Therefore, there is an urgent need to develop an innovatory and convenient sensor that is capable of detecting the presence of parts-per-billion level Hg^{2+} ions in water.

A promising way is to develop optical chemosensors for detecting Hg^{2+}, based on an indicator that is capable of reporting on the selectivity recognition of Hg^{2+} through optical responses. Among the numerous indicators, pyrene derivatives are widely used as fluorescence indicators in optical sensors because they have many advantages, such as large Stokes shift, high quantum yield, excellent photostability, and no toxicity [15–20].

Recently, functionalized mesoporous materials have received much attention and have been proved to be excellent host materials for developing functional materials because of their high surface area, uniform porosity, and low absorption and emission in visible spectrum [21–23]. Mesoporous bulk MCM-41and SBA-15 are usually used as a support for fluorescence indicators. Our research team previously reported a novel fluorescent chemosensing hybrid material prepared by covalently grafting Py-OH to bulk mesoporous silica SBA-15 for detecting Hg^{2+} in water [17]. However, it may be difficult for Hg^{2+} to disperse quickly into the mesoporous channel, resulting in the unsatisfied detection limit and long response time. Based on above considerations, we propose some improvements to make the channel distributed only onto the surface of the support, looking forward to improve results.

In this paper, we propose a strategy for the fabrication of a low cost, high sensitivity, high selectivity, and well monodispersed

* Correspondence to: Key Laboratory of Excited State Processes, Changchun Institute of Optics, Fine 16 Mechanics and Physics, Chinese Academy of Sciences, 3888 Eastern South-Lake 17 Road, Changchun 130033, P. R. China.
Fax: +86 431 86176935.
E-mail address: lib020@yahoo.cn (B. Li).

0022-2313/$ - see front matter © 2012 Elsevier B.V. All rights reserved.
doi:10.1016/j.jlumin.2012.01.049

core–shell structured pyrene functionalization of mesoporous silica. Spherical SiO_2 is used as the core and ordered mesoporous silica as the shell, which is further functionalized by the pyrene derivative as a fluorescence indicator. The detection of Hg^{2+} is based on the fluorescence intensity changes of the sensor, with a limit detection of 3.4×10^{-9} g mL^{-1}. Moreover, it also demonstrates a high selectivity for Hg^{2+} in the presence of other metal ions such as Na^+, K^+, Ag^+, Mg^{2+}, Ca^{2+}, Ba^{2+}, Cu^{2+}, Zn^{2+}, Cd^{2+}, and Pb^{2+}. Based on these results, a highly selective and sensitive optical chemosensor for Hg^{2+} determination is successfully developed.

2. Materials and methods

2.1. Materials

Analytical grade solvents and compounds were used for preparation. Tetraethoxysilane (TEOS, Tianjin Chemicals Co.), 3-(triethoxysilyl)-propyl isocyanate (TESPIC, Aldrich), 4-hydroxy-benzaldehyde (Aldrich), and 1-pyrenecarboxaldehyde (Aldrich) were used as received. Mercury nitrate and the other inorganic metal salts were purchased from Shanghai Chemical Company (Shanghai, China). The solvent toluene was used after desiccation with anhydrous sodium sulfate (Beijing, China). Concentrated HCl, $NH_3\cdot H_2O$, and ethanol were obtained from Beijing Chemical Company. The water used in our present work was deionized.

2.2. Synthetic procedures

2.2.1. Synthesis of the alkoxysilane modified pyrene (denoted as Py-Si)

The synthetic procedure of Py-Si is shown in Scheme 1. The alkoxysilane modified pyrene (Py-Si) was synthesized by modifying a reported procedure [24]. Firstly, 1-(4–hydroxyphenyl)-4-pyrenyl-2,3-diaza-1,3-butadiene (Py-OH) was obtained as a starting material following the literature procedure [17]. Then, 1 mmol of Py-OH was mixed with 6.37 mmol of TESPIC, which was dissolved in 20 mL chloroform in a round-bottom flask, and the mixture was stirred under N_2 atmosphere at 60 °C for 72 h. Then cold hexane was added dropwise into the flask to precipitate a yellow solid from the mixture. The final filtered-off precipitate was washed with several portions of cold hexane, then eliminated by evaporation, and dried in vacuo. Py-Si: IR –CONH 1510 cm^{-1}, 1695 cm^{-1}, Si–O 1083 cm^{-1} (ν_{as}, Si–O), and 803 cm^{-1}(ν_s, Si–O).

2.2.2. Synthesis of the core–shell mesoporous silica

SiO_2 nanoparticles were firstly prepared following the well-known modified Stöber method [25]. The core–shell mesoporous silica was prepared according to the previous report with some modifications [26]. 0.05 g SiO_2 was well dispersed in the mixture solution of 0.15 g cetyltrimethylammonium bromide (CTAB), 40 mL deioned water, 0.5 g concentrated ammonia aqueous solution (28 wt%), and 30 mL ethanol. After the solution was stirred for 0.5 h, 0.40 g TEOS was added dropwise to the solution with vigorous stirring. After reaction for 6 h, the product was collected by centrifugation and washed several times with ethanol and water. The above coating process was repeated twice. The structure-directing agent (CTAB) was removed by acid/solvent extraction, using a solution of 1 M HCl in ethanol. This mixture was refluxed for 72 h, then filtered and washed with EtOH to remove the residual HCl. The product was dried at 60 °C for 12 h in vacuo to obtain the synthesized core–shell mesoporous silica.

2.2.3. Synthesis of pyrene functional core–shell structured mesoporous silica material (denoted as SiO_2@mSiO_2/Py-Si)

Synthetic procedures of SiO_2@mSiO_2/Py-Si are shown in Scheme 2. The target product was prepared via a reported synthesis route with some modifications [27]. Py-Si and activated core–shell mesoporous silica (1:1 mass ratio) were refluxed with anhydrous toluene for 48 h under an N_2 atmosphere. The resulting product was collected by centrifugation and washed several times with ethanol. Finally, the product was dried in a vacuum oven.

2.3. Characterization

The IR absorption spectra were measured in the range 400–4000 cm^{-1} using a FT-IR spectrophotometer (model Bruker Vertex 70 FT-IR) with a resolution of ±4 cm^{-1} using the KBr pellet technique. The fluorescencence emission spectra were recorded at room temperature with a Hitachi F-4500 spectrophotometer equipped with a continuous 150 W Xe-arc lamp. Small-angle X-ray diffraction (SAXRD) analysis was performed with a Rigaku-Dmax 2500 diffracrtometer using Cu Kα_1 (λ=0.154 05 nm) radiation with scanning step of 0.02° (2θ). Field-emission scanning electron microscopy (FE-SEM) images were measured on a Hitachi S-4800 microscope. Thermogravimetric analysis (TGA) was performed on 2 mg of samples using a Perkin-Elmer thermal analyzer. The sample was heated from 40 to 600 °C at a heating rate of 10.0 °C min^{-1}. A 10 mL min^{-1} flow of dry nitrogen was used to purge the sample at all times. All spectrophotometric

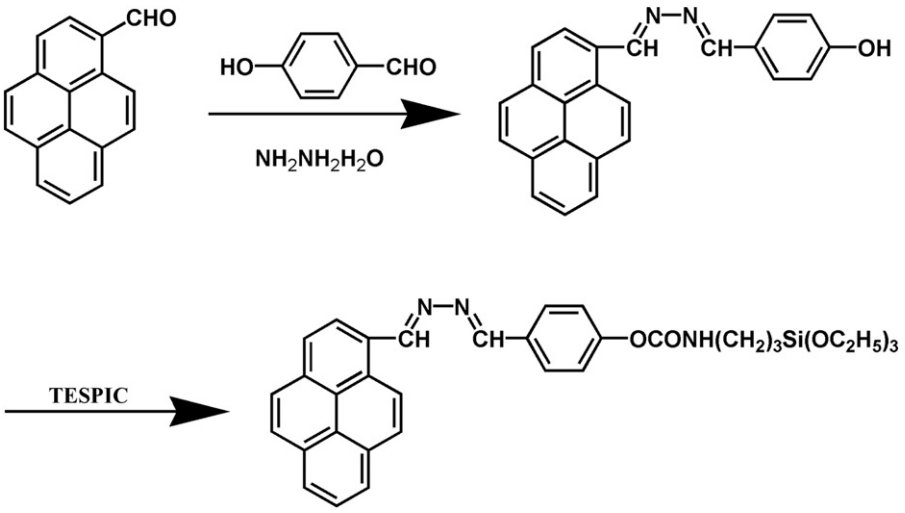

Scheme 1. Synthesis of the alkoxysilane modified pyrene Py-Si.

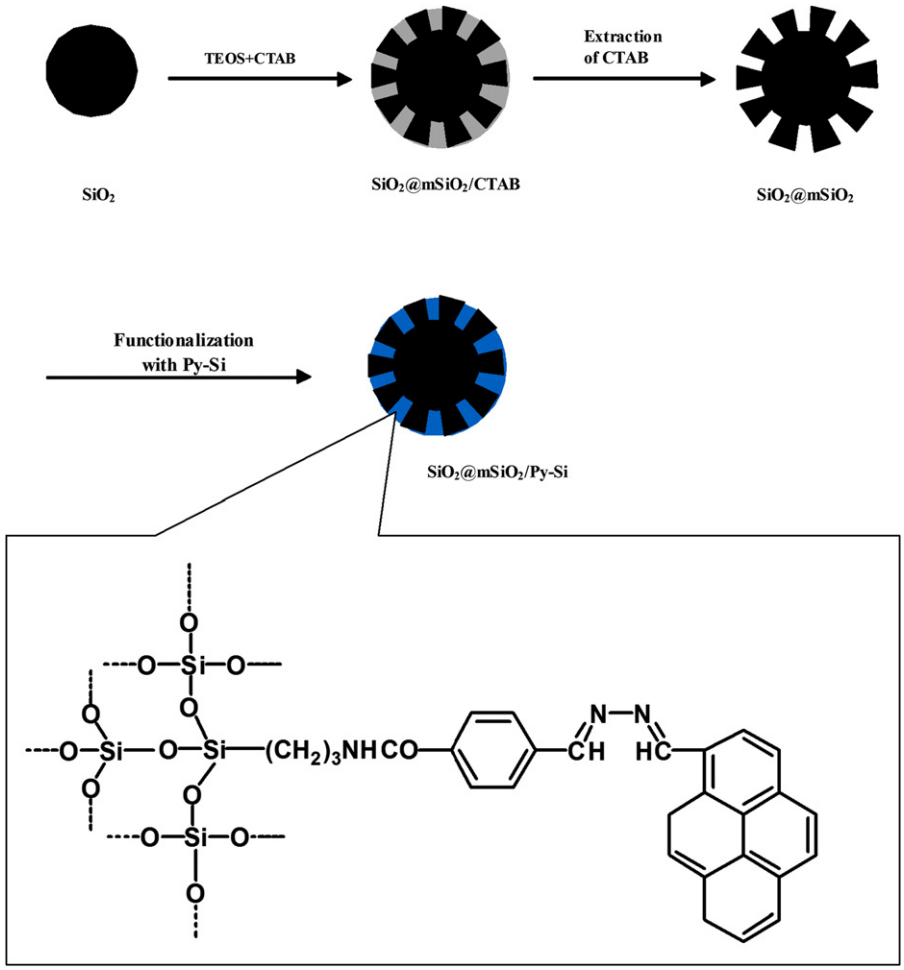

Scheme 2. Formation of the SiO_2@mSiO_2/Py-Si.

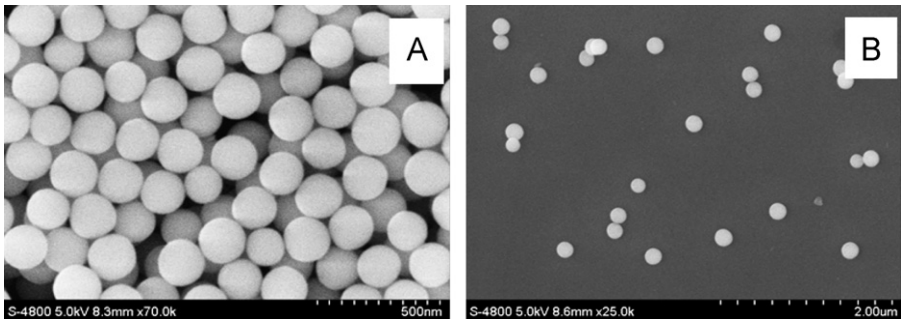

Fig. 1. SEM images of SiO_2 nanospheres (A) and core–shell structured mesoporous silica SiO_2@ mSiO_2 (B).

spectra of the mesoporous silica material were performed with a suspension of sample dispersed in deionized water and then brought into a quartz cell for measurement. The concentrations of Hg^{2+} in real samples from different sources were determined with a Leeman Prodigy Inductively Coupled Plasma Atomic Emission Spectrometry (ICP-AES).

3. Results and discussion

3.1. SEM images

Fig. 1 shows the SEM images of the SiO_2 nanoparticles and core–shell structured mesoporous silica (SiO_2@mSiO_2). It can be observed that the SiO_2 nanoparticles with a mean diameter of 185 nm are uniform and monodispersed, making the next coating procedure possible. The obtained SiO_2@mSiO_2 has a mean diameter of 208 nm, which is larger than that of SiO_2 nanoparticles, indicating that SiO_2 nanoparticles are successfully coated by mesoporous silica shell with a thickness of 23 nm through the sol–gel approach.

3.2. Small-angle XRD patterns

X-ray diffraction patterns of SiO_2@mSiO_2 (a) and the SiO_2@m-SiO_2/Py-Si (b) are presented in Fig. 2. SiO_2@mSiO_2 exhibits three well-resolved broad Bragg reflections, consisting of a strong (1 0 0) peak reflection in a low angle region ranging from 1° to 2.5° (2θ) and two low (1 1 0) and (2 0 0) peak reflections located in a higher

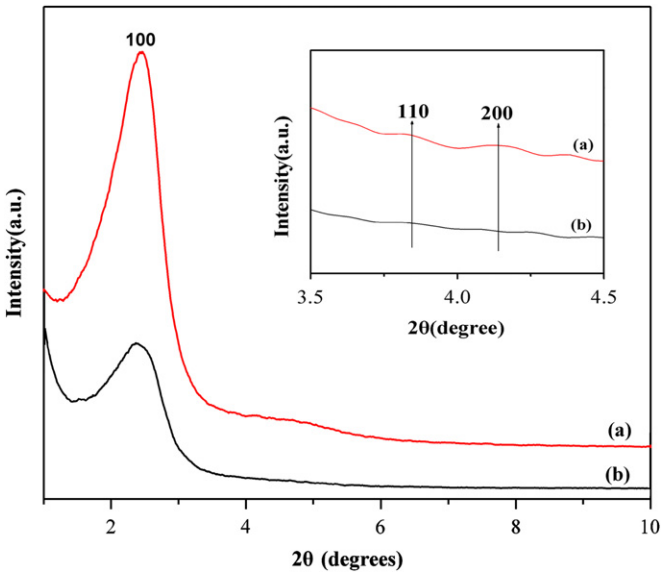

Fig. 2. Low-angle XRD patterns of SiO_2@mSiO_2 (a) and the SiO_2@mSiO_2/Py-Si (b).

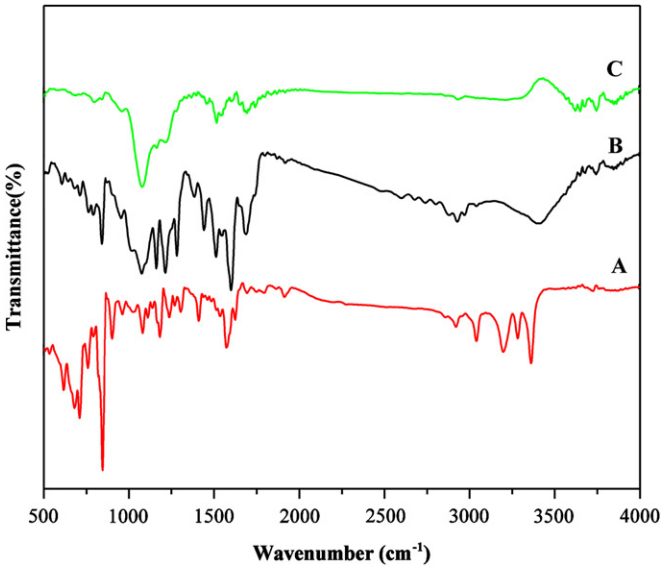

Fig. 3. FT-IR spectra of Py-OH (A), Py-Si (B), and SiO_2@mSiO_2/Py-Si (C).

angle range of 3.5–4.5° (2θ), confirming its ordered mesoporous structure. SiO_2@mSiO_2/Py-Si shows a similar pattern, suggesting the maintenance of the mesoporous structure after functionalization. However, it is worth noting that SiO_2@mSiO_2/Py-Si shows a different diffraction intensity compared with that of non-functional SiO_2@mSiO_2. The presence of organic component covalently grafted into the pore channels may decrease the mesoscopic order of the pore channels, leading to the decreased intensity of (1 0 0) (1 1 0), and (2 0 0) peaks. The unit-cell parameter (a_0) is calculated to be 4.227 nm for SiO_2@mSiO_2 and 4.165 nm ($d_{100}=\lambda/2\sin\theta$, $a_0=2d_{100}/\sqrt{3}$) for SiO_2@mSiO_2/Py-Si according to the literature method [28]. The similar unit-cell parameter further confirms that the ordered hexagonal framework of SiO_2@mSiO_2/Py-Si has been preserved after the introduction of Py-Si.

3.3. FT-IR spectra

The presence of Py-Si covalently bonded onto the mesoporous silica is characterized by IR spectroscopy (Fig. 3), where A, B, and C stand for Py-OH, Py-Si, and SiO_2@mSiO_2/Py-Si, respectively. The absorption band at 3357 cm^{-1} in Fig. 3(A) is assigned to the strong vibration of hydroxyl. The emergence of a series of bands at 2970, 2929, and 2881 cm^{-1} owing to the vibrations of methylene–$(-CH_2)_3-$, along with the appearance of the peaks located at 1510, 1695 cm^{-1} in Fig. 3(B) and (C) corresponding to the –CONH– group, proves that Py-OH has been successfully grafted on to TESPIC. The peaks located at 1083 cm^{-1} (*vas*, Si–O), 803 cm^{-1} (*vs*, Si–O), and 465 cm^{-1} (δ, Si–O–Si) (v represents stretching, δ in plane bending, *s* symmetric, and *as* asymmetric vibrations) in Fig. 3(C) are attributed to the absorption of siloxane bonds, which confirms the formation of Si–O–Si framework. These results suggest that Py-Si is successfully grafted into the channels of mesoporous silica.

3.4. Thermogravimetric analysis

Thermogravimetric analysis of the SiO_2@mSiO_2/Py-Si is carried out under N_2 atmosphere with a heating rate of 10 °C min^{-1}. As shown in Fig. 4, the TGA curve exhibits a three-step degradation process: the first step degradation is observed in the region from 20 to 100 °C, the second one appears from 170 to 340 °C, and the last one occupies a region from 400 to 600 °C. The first weight loss is assigned to the thermal release of physisorbed water molecules. The decomposition of organic moiety should be responsible for the second weight loss. The third weight loss is then attributed to the thermal degradation of organosilicate frameworks, including Si–C, C–C, and C–N bond cleavages [29]. Usually, measurements are taken at room temperature, and from the above results, we know that SiO_2@mSiO_2/Py-Si has a wonderful thermal stability below 100 °C. Therefore, SiO_2@mSiO_2/Py-Si can provide desirable thermal stability for practical applications as a fluorescent sensor. From the second weight loss, the amount of organic moiety immobilizing onto the mesoporous silica is estimated to be about 14%.

3.5. Fluorescence spectra

3.5.1. Selectivity of SiO_2@mSiO_2/Py-Si

The selectivity of SiO_2@mSiO_2/Py-Si towards metal ions is investigated (Fig. 5) by interaction with 10^{-3} M of representative alkali (Na^+, K^+), alkaline earth (Mg^{2+}, Ca^{2+}, and Ba^{2+}), and transition-metal ions (Ag^+, Cu^{2+}, Pb^{2+}, Zn^{2+}, Cd^{2+}, and Hg^{2+}). From Fig. 5, it can be observed that the fluorescence intensity of SiO_2@mSiO_2/Py-Si enhances significantly only in the presence

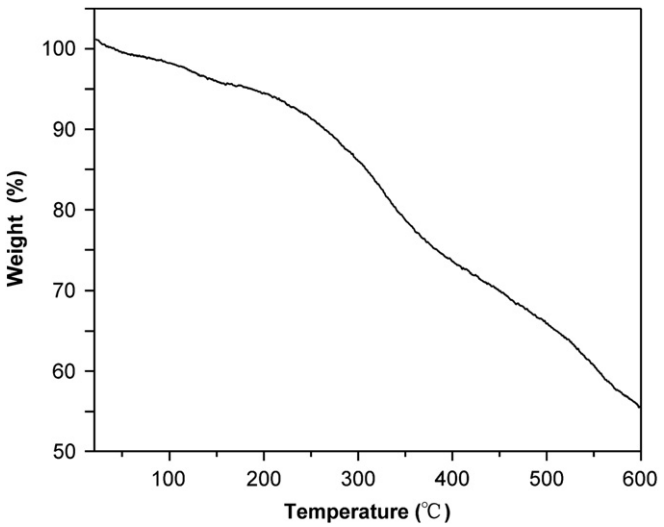

Fig. 4. Thermogravimetric analysis data of SiO_2@mSiO_2/Py-Si.

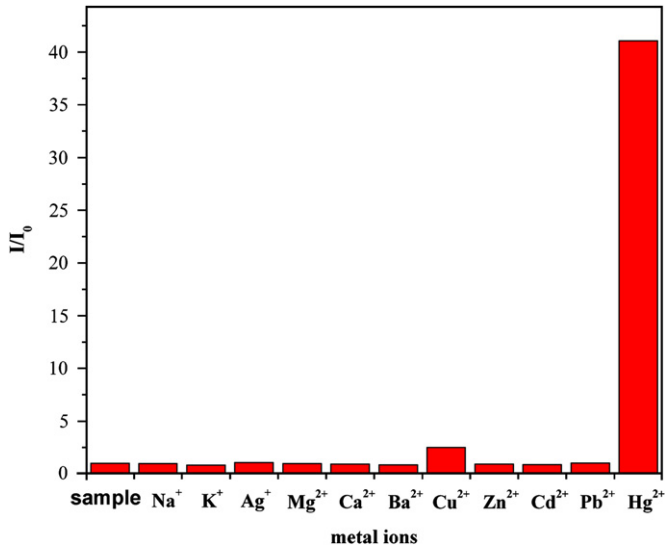

Fig. 5. The fluorescence response I/I_0 of SiO_2@mSiO_2/Py-Si towards metal ions (λ_{ex}=350 nm, λ_{em}=380 nm).

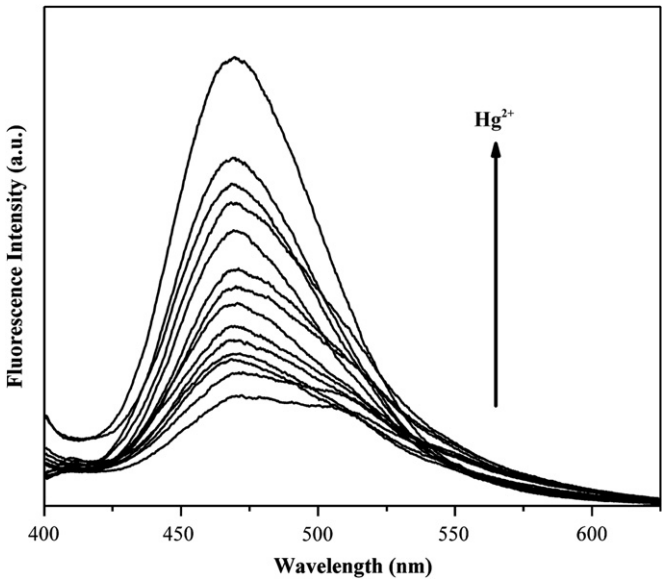

Fig. 6. Fluorescence spectra (λ_{ex}=350 nm) of the SiO_2@mSiO_2/Py-Si (1.6 mg/5 mL) in deionized water with increasing amounts of Hg^{2+} (10^{-8}–10^{-4} M).

of Hg^{2+}. Upon the addition of above-mentioned ions, the fluorescence intensity of SiO_2@mSiO_2/Py-Si changes slightly. This result indicates that SiO_2@mSiO_2/Py-Si can recognize Hg^{2+} from other metal ions. The good selectivity of SiO_2@mSiO_2/Py-Si towards Hg^{2+} makes it a promising candidate for applications in environment protection.

3.5.2. *Sensitivity of SiO_2@mSiO_2/Py-Si*

To further explore the availability of SiO_2@mSiO_2/Py-Si as a novel fluorescence chemosensor for Hg^{2+}, the fluorescence response profiles of SiO_2@mSiO_2/Py-Si (1.6 mg/5 mL) are recorded at room temperature upon gradual addition of small amounts of Hg^{2+} into suspended SiO_2@mSiO_2/Py-Si aqueous solutions. Fig. 6 gives the detailed fluorescence changes of SiO_2@mSiO_2/Py-Si upon different concentrations of Hg^{2+} under the same condition. In absence of Hg^{2+}, the fluorescence emission intensity of SiO_2@mSiO_2/Py-Si is very weak. Upon the increasing concentration of Hg^{2+}, a significant enhancement of the characteristic fluorescence of pyrene emerges at 470 nm, and we are giving the sensing mechanism of Hg(II) with functionalized material as follows. In the absence of Hg^{2+}, the lone pair electrons of the nitrogen atoms are transferred to the pyrene which is electron-deficient, resulting in the quenching of the pyrene emission in the free state [30]. By adding Hg^{2+} into the suspension of SiO_2@mSiO_2/Py-Si, the lone pairs may enter into an empty orbit (d) of Hg^{2+} but no longer participate in the quenching process, causing the recovery of the fluorescence. From Fig. 6, we also note that SiO_2@mSiO_2/Py–Si has a good sensitivity towards Hg^{2+} with a detection limit of 3.4×10^{-9} g mL^{-1} under current experimental conditions. This parameter is 100 times lower (down to the ppb level) than our previous report of covalently grafted Py-Si onto the bulk mesoporous silica SBA-15 [17]. The excellent sensitivity of SiO_2@mSiO_2/Py-OH can be ascribed to improvement of channel distribution, and the channels of SiO_2@mSiO_2/Py-Si distribute only on the surface of the support, which facilitates the entry of Hg^{2+}.

3.5.3. *Linear spectral response of SiO_2@mSiO_2/Py-Si*

The fluorescence response plot of SiO_2@mSiO_2/Py–Si exhibits a linear response (R^2=0.9913) over the concentration range of 10^{-4}–10^{-8} M as shown in Fig. 7. A good linear response towards Hg^{2+} in a wider range indicates that the fluorescence intensity of SiO_2@mSiO_2/Py-Si changes regularly in specific concentration

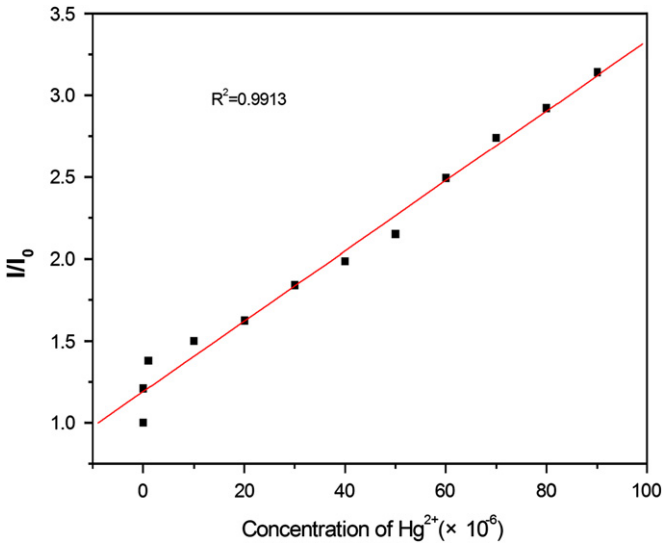

Fig. 7. Plot of fluorescence response I/I_0 of SiO_2@mSiO_2/Py-Si (1.6 mg/5 mL) with increasing amounts of Hg^{2+} from 10^{-8} to 10^{-4} M in deionized water (λ_{ex}=350 nm and λ_{em}=380 nm).

range, suggesting that SiO_2@mSiO_2/Py-Si has a potential application in environmental monitoring.

3.5.4. *Recognition of Hg^{2+} in a real sample*

We got some water from SongHua River as a real sample, to test the practical implementation of SiO_2@mSiO_2/Py-Si in the detection of Hg^{2+}. The sample was tested by ICP-AES and SiO_2@mSiO_2/Py-Si. The analytical data are listed in Table 1. There is a small deviation between the amounts of Hg^{2+} determined by SiO_2@mSiO_2/Py-Si and by ICP-AES. This result may be caused by other heavy metal ions which are also in the river and can interact with SiO_2@mSiO_2/Py-Si.

4. Conclusions

In summary, we have designed and synthesized a pyrene functional core–shell structured mesoporous silica material as a

Table 1
Recognition of Hg^{2+} in real samples. Data marked [a] are obtained by ICP-AES, and data marked [b] are obtained by SiO_2@mSiO_2/Py-Si.

Sample	The Amount of [a]Hg(II) [μmol/L]	The Amount of [b]Hg(II) [μmol/L]
Water from river	0.15	1.089

novel fluorescent chemosensor for detecting Hg^{2+}. The amount of organic moiety immobilizing onto the core–shell structured mesoporous silica is about 14%, indicating that the core–shell structured mesoporous silica is a wonderful support for fluorescence indicators. The fluorescence intensity of SiO_2@mSiO_2/Py-Si enhances with increasing concentrations of Hg^{2+}, which is attributed to the complexation of SiO_2@mSiO_2/Py-Si with Hg^{2+}. And because of the improvement of channel distribution, SiO_2@mSiO_2/Py-Si shows a linear response (R^2=0.9913) towards Hg^{2+} in the concentration range of 10^{-8}–10^{-4} M with a satisfactory detection limit of 3.4×10^{-9} g mL^{-1}. Moreover, SiO_2@mSiO_2/Py-Si exhibits a high selectivity towards Hg^{2+}. The high selectivity, excellent sensitivity, and the simple preparation method endow this novel fluorescent chemosensor with the potential for application in detection of Hg^{2+} in water.

Acknowledgments

The authors gratefully thank the financial supports of the National Natural Science, Foundations of China (Grant Nos 51172224 and 51103145), the Science and Technology Developing Project of Jilin Province (Grant no. 20100533), and the Fundamental Research Funds for the Central Universities.

References

[1] A. Renzoni, F. Zino, E. Franchi, Environ. Res. Sect. A 77 (1998) 68.
[2] P.B. Tchounwou, W.K. Ayensu, N. Ninashvili, D. Sutton, Environ. Toxicol. 18 (2003) 149.
[3] D.W. Boening, Chemosphere 40 (2000) 1335.
[4] I. Hoyle, R.D. Handy, Aquat. Toxicol. 72 (2005) 147.
[5] R.K. Zalups, Pharmacol. Rev. 52 (2000) 113.
[6] A.B. Kobal, M. Horvat, M. Prezelj, A.S. Briški, M. Krsnik, T. Dizdarevič, D. Mazej, I. Falnoga, V. Stibilj, N. Arnerič, D. Kobal, J. Osredkar, J. Trace Elem. Med. Biol. 17 (2004) 261.
[7] Y.A. Vil'pan, I.L. Grinshtein, A.A. Akatove, S. Gucer, J. Anal. Chem 60 (2005) 45.
[8] E. Kopysc, K. Pyrzynska, S. Garbos, E. Bulska, Anal. Sci. 16 (2000) 1309.
[9] D. Karunasagar, J. Arunachalam, S. Gangadharan, J. Anal. At. Spectrom. 13 (1998) 679.
[10] L. Yu, X. Yan, At. Spectrom. 25 (2004) 145.
[11] M.J. Bloxham, S.J. Hill, P.J. Worsfold, J. Anal. At. Spectrom. 11 (1996) 511.
[12] C.A. Trimble, R.W. Hoenstine, A.B. Highley, J.F. Donoghue, P.C. Ragland, Mar. Georesour. Geotechnol. 17 (1999) 187.
[13] T. Smigelski, K. O'Brien, J. Fusco, J.C. Schaumloffel, J. Tausta, Proceedings of the 226th ACS National Meeting, September 7–11, 2003.
[14] X. Yin, Q. Xu, X. Xu, Fenxi Huaxue 23 (1995) 1168.
[15] X. Wang, C. Drew, S.H. Lee, K.J. Senecal, J. Kumar, L.A. Samuelson, Nano Lett. 2 (2002) 1273.
[16] S.H. Lee, J. Kumar, S.K. Tripathy, Langmuir 16 (2000) 10482.
[17] Y.H. Wang, B. Li, L.M. Zhang, Li.N. Liu, Q.H. Zuo, P. Li, New J. Chem. 34 (2010) 1946.
[18] C. Díez-Gil, R. Martínez, I. Ratera, A. Tárraga, P. Molina, J. Veciana, J. Mater. Chem. 18 (2008) 1997.
[19] M. Kumar, A. Dhir, V. Bhalla, R. Sharma, R.K. Puri, R.K. Mahajan, Analyst 135 (2010) 1600.
[20] A. Caballero, R. Martínez, V. Lloveras, I. Ratera, J. Vidal-Gancedo, K. Wurst, A. Tárraga, P. Molina, J. Veciana, J. Am. Chem. Soc. 127 (2005) 15666.
[21] B.J. Scott, G. Wirnsberger, G.D. Stucky, Chem. Mater. 13 (2001) 3140.
[22] J. Tan, H.F. Wang, X.P. Yan, Anal. Chem. 81 (2009) 5273–5280.
[23] M. Colilla, I.I. Barba, S.S. Salcedo, José L.G Fierro, José L. Hueso, M.V. Regí, Chem. Mater. 22 (2010) 6459.
[24] B.F. Lei, B. Li, H.R. Zhang, S.Z. Lu, Z.H. Zheng, W.L. Li, Y. Wang, Adv. Funct. Mater. 16 (2006) 1883.
[25] W. Stöber, A. Fink, E. Bohn, J. Colloid Interface Sci. 26 (1968) 62.
[26] P.P. Yang, Z.W. Quan, Z.Y. Hou, C.X. Li, X.J. Kang, Z.Y. Cheng, J. Lin, Biomaterials 30 (2009) 4786.
[27] T. Balaji, M. Sasidharan, H. Matsunaga, Analyst 130 (2005) 1162.
[28] F. Chen, Y.P. Zhu, H.L. Ma, Z.L. Bo, J.L. Zhang, Acta Phys.Chim.Sin. 20 (2004) 1292.
[29] T. Tien, L.K. Chau, Chem. Mater. 11 (1999) 2141.
[30] S.R. Davidson, Adv. Phys. Org. Chem. 19 (1983) 1.